

Structure of the Jet-Cooled 1-Naphthol Dimer Studied by IR Dip Spectroscopy: Cooperation between the π – π Interaction and the Hydrogen Bonding

Morihisa Saeki

Quantum Beam Science Directorate, Japan Atomic Energy Agency, Tokai-mura, Naka-gun, Ibaraki 319-1195, Japan

Shun-ichi Ishiuchi, Makoto Sakai, and Masaaki Fujii*

Chemical Resources Laboratory, Tokyo Institute of Technology, 4259 Nagatsuta, Midori-ku, Yokohama 226-8503, Japan

Received: October 20, 2006; In Final Form: December 8, 2006

The structure of a jet-cooled 1-naphthol (1-NpOH) dimer was investigated by using resonant-enhanced two-photon ionization (R2PI) and ion-detected infrared (IR) dip spectroscopy. A geometrical optimization and a frequency calculation in (1-NpOH)₂ were also performed at the MP2/cc-pVDZ level. Stable isomers in the MP2/cc-pVDZ calculation were classified into a structure dominated only by the π – π interaction and structures formed by cooperation between the π – π interaction and hydrogen bonding. On the basis of a comparison between the observed and calculated IR spectra, the geometry of (1-NpOH)₂ was concluded to be a π – π stacking structure supported by hydrogen bonding.

I. Introduction

Cooperation between the π – π interaction (also called the stacking interaction) and the hydrogen bonding often plays a key role in the formation of biological systems and organic crystals. For example, the double-stranded secondary structure of DNA is held together by the π – π interaction and the hydrogen bonding between the nearest-neighbor bases on opposite strands.¹ These interactions induce the coupling of adenine with thymine and that of guanine with cytosine. To elucidate the built-up mechanism of the biological system, we need to obtain information about the cooperation between the π – π interaction and the hydrogen bonding. For this purpose, many researchers have investigated the structure of clusters of nucleobases by ab initio MO calculations^{2–6} and spectroscopic techniques.^{7–10} Recently Hobza and co-workers have revealed by advanced theoretical studies that the π – π stacking interaction is strong enough to compete with hydrogen bonding in nucleobase clusters.^{4,5} This clearly shows the importance of the π – π stacking/hydrogen-bonding cooperation. To know the π – π stacking/hydrogen-bonding cooperation in detail, we are motivated to study the cooperation in a simpler benchmark. A cluster of aromatic hydroxyl compounds (ArOH), such as phenol and naphthol, is a simple model for studying the cooperation between two kinds of interactions, because they have both aromatic rings available for the π – π interaction and hydroxyl groups for the hydrogen bonding. Studies on the phenol dimer (PhOH)₂, however, have suggested that the structure is mainly dominated by the hydrogen bonding, and is not affected by the π – π interaction.^{11–17} The cluster of phenol is inadequate to study the cooperation between the π – π interaction and the hydrogen bonding because of the weak π – π interaction.

In clusters of ArOH with its larger aromatic ring, the π – π interaction is assumed to be more crucial. In this study, we

investigated the structure of the 1-naphthol dimer (1-NpOH)₂ by resonant two-photon ionization (R2PI) and ion-detected infrared (IR) dip spectroscopy. For the analysis of the experimental results, the geometrical optimization and frequency calculation in (1-NpOH)₂ were performed at the MP2/cc-pVDZ level. From a comparison of the observed IR spectrum with the calculated ones of the optimized isomers, we concluded that the geometry of (1-NpOH)₂ is the stacking structure supported by the hydrogen bonding. This conclusion is consistent with the difference in the geometrical structures and the vibrational spectra between (1-NpOH)₂ and (PhOH)₂.

II. Methods

A. Experimental Methods. Parts of the experimental apparatus are shown in Figure 1. The chamber was designed to obtain a high pumping speed, which helps to form large clusters. The (1-NpOH)₂ cluster was generated by passing 7 atm of neon gas through an internal heated reservoir of 1-NpOH (100–120 °C) in a pulsed nozzle (Even-Lavie valve system, 250 μ m diameter orifice¹⁸) operated at 20 Hz. The source chamber was evacuated at a speed of 2700 L/s by three turbo pumps (Alkatel ATP900). The pressure of the chamber increased from $\sim 5 \times 10^{-8}$ to $\sim 4 \times 10^{-6}$ Torr when the gas was on. The cluster beam was skimmed into a second vacuum chamber and was ionized by ultraviolet laser pulses. The ionized cluster was extracted at 10 cm downstream from the valve perpendicularly to the initial beam direction by applying an electronic field of 2.8 kVcm⁻¹. The cluster ion was further accelerated up to 7 kV and introduced into a microchannel plate (BURLE Model 3040MA) through several ion optics. The high-voltage acceleration in the TOF mass spectrometer enabled us to effectively detect any large and heavy clusters.

The setup of the laser system for the R2PI and IR dip spectroscopy has been described elsewhere.^{19–21} Briefly, the S₁←S₀ R2PI spectrum was measured by monitoring the intensity

* Address correspondence to this author. Phone/Fax: +81-45-924-5250. E-mail: mfujii@res.titech.ac.jp.

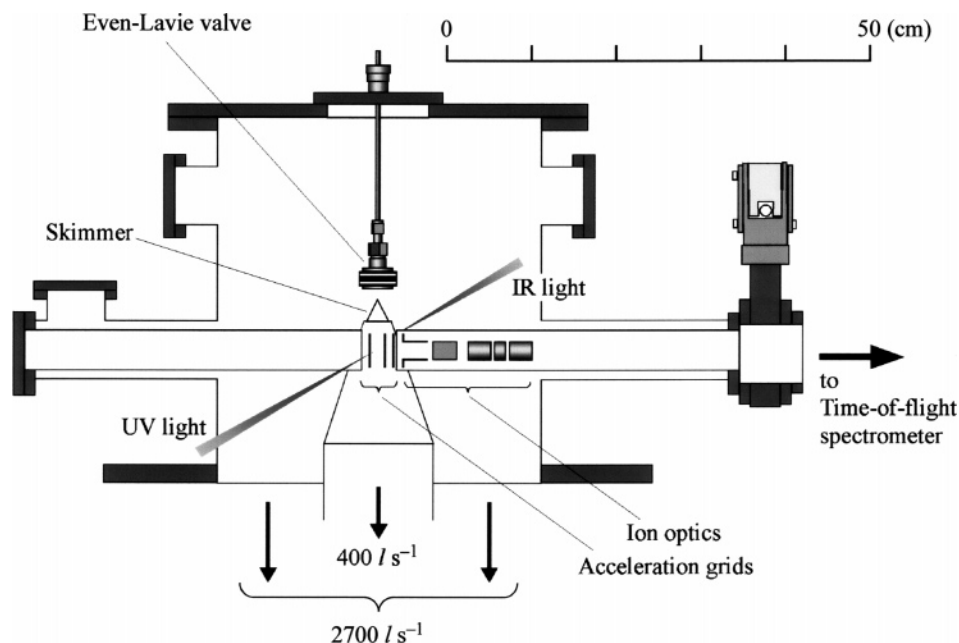


Figure 1. Parts of the experimental apparatus for the preparation, ionization, and acceleration of the clusters.

of ions of $(1\text{-NpOH})_2$ as a function of the wavelength of the laser. In IR dip spectroscopy, the IR laser pulse was irradiated to the $(1\text{-NpOH})_2$ prior to irradiation by the ionization laser, of which the wavelength was fixed to the origin band of the $S_1 \leftarrow S_0$ transition. By monitoring the intensity of the ions of $(1\text{-NpOH})_2$, the wavelength of infrared light was scanned. When the frequency of the IR light matched the transition to a certain vibrational level, the ion current decreased because of a loss of population from the ground vibrational state. Thus, the IR absorption can be detected by depletion of the ion current.

Regarding this experiment, we would like to note that the contamination of a mixed cluster of 1-naphthol dimer with water $(1\text{-NpOH})_2(\text{H}_2\text{O})_n$ must be avoided. The existence of traces of water in a sample line results in the formation of the $(1\text{-NpOH})_2(\text{H}_2\text{O})_n$ cluster, which can appear as $(1\text{-NpOH})_2^+$ ions by the evaporation of water molecules after ionization. The $(1\text{-NpOH})_2^+$ ions originating from $(1\text{-NpOH})_2(\text{H}_2\text{O})_n$ make the $S_1 \leftarrow S_0$ R2PI spectrum of $(1\text{-NpOH})_2$ structureless. Thus, complete dehydration is essential for observing the structured spectrum of the pure $(1\text{-NpOH})_2$ cluster.

B. Calculation. The program used was the GAUSSIAN 03 package.²² We performed geometrical optimization and a frequency calculation on $(1\text{-NpOH})_2$ at the MP2/cc-pVDZ level. The MP2/cc-pVDZ calculation is adequate for a qualitative estimate of the π - π interaction and the hydrogen bonding.^{5,6,23-25} The initial structures of $(1\text{-NpOH})_2$ were prepared by substituting OH groups for the 1-position H atoms in the naphthalene dimers, as described in our previous paper.²³ The molecular structures of $(1\text{-NpOH})_2$ were optimized by using an energy-gradient technique for the MP2 method with the usual frozen-core approximation. The stability of the optimized structures was checked by a harmonic frequency analysis. If the optimized structure had one or more imaginary frequencies with fixed symmetry, it was re-optimized with the lower symmetry. The procedure was iterated until the true local minimum structure was obtained. In estimating the binding energy of the dimer, BSSE was corrected by using the counterpoise (CP) method.²⁶ The frequency and its IR intensity were calculated with the Freq=Numerical option. All of the computations were carried out on a NEC SX-7 computer at the Research Center for Computational Science, Okazaki, Japan.

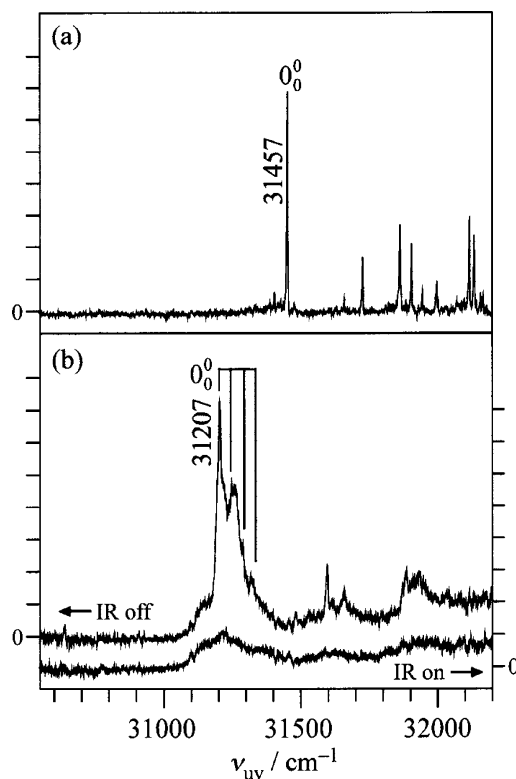


Figure 2. $S_1 \leftarrow S_0$ R2PI spectra of (a) 1-NpOH and (b) $(1\text{-NpOH})_2$. The origin band is at 31457 cm^{-1} in part a and at 31207 cm^{-1} in part b. The lower trace in part b indicates the $S_1 \leftarrow S_0$ R2PI spectrum with IR light in the IR-UV hole-burning process.

III. Results and Discussion

A. $S_1 \leftarrow S_0$ R2PI Spectrum of $(1\text{-NpOH})_2$. The $S_1 \leftarrow S_0$ R2PI spectrum in the region from 30550 to 32200 cm^{-1} is shown in Figure 2a for 1-naphthol monomer 1-NpOH and in Figure 2b for the dimer $(1\text{-NpOH})_2$. The 1-NpOH molecules have *trans* and *cis* isomers.²⁷⁻²⁹ Figure 2a shows the origin band of *trans*-1-NpOH at 31457 cm^{-1} . The *cis*-1-NpOH isomer, of which the origin was assigned to 31181 cm^{-1} ,²⁷ was negligible under the present condition. The vibronic bands in Figure 2a are assigned

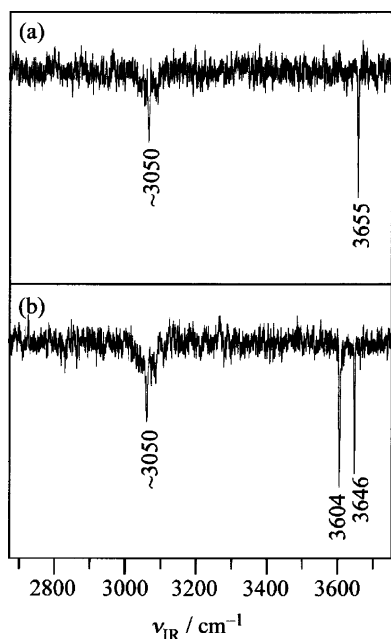


Figure 3. Ion-detected IR dip spectra of (a) 1-NpOH and (b) (1-NpOH)₂. The UV laser was fixed at the origin bands of each species.

to a $L_b \pi-\pi^*$ transition.^{29,30} The $S_1 \leftarrow S_0$ R2PI spectrum of (1-NpOH)₂ maintains the vibronic structure in the spectrum of 1-NpOH and shows a broadening of the bandwidth. The bands around 31207 cm⁻¹ show a partially resolved progression with four evident peaks, which are separated by 37–45 cm⁻¹. The lowest band at 31207 cm⁻¹ is assigned to the origin band of (1-NpOH)₂. The progression is assignable to the intermolecular vibration of (1-NpOH)₂ in the S_1 state because it is not observed in the 1-NpOH monomer. The appearance of the vibrational structure in the intermolecular mode means that the intermolecular conformation is weakly distorted by photoexcitation.

B. IR Dip Spectrum of (1-NpOH)₂. The IR dip spectrum in the region from 2670 to 3750 cm⁻¹ is shown in Figure 3a for *trans*-1-NpOH and in Figure 3b for (1-NpOH)₂. The UV laser was fixed at the $S_1 \leftarrow S_0$ origins (31457 and 31207 cm⁻¹ for 1-NpOH and (1-NpOH)₂, respectively). To examine the coexistence of the isomers, we applied IR–UV hole-burning spectroscopy to (1-NpOH)₂. This method is a kind of population labeling spectroscopy to extract those electronic transitions contributing to a single species. The detailed principle of IR–UV hole-burning spectroscopy has been described elsewhere.²¹ By fixing the IR laser frequency to 3604 cm⁻¹ with the highest power, we scanned the UV frequency over the energy range for the $S_1 \leftarrow S_0$ transition. The lower trace in Figure 2b shows the IR–UV hole-burning spectrum. The sharp vibronic bands disappeared when the IR laser was introduced. The result indicates that no isomer coexisted under the present condition, unless the isomers would have had the same vibrational frequency.

The vibrational bands in 1-NpOH around 3050 cm⁻¹ are assignable to the CH stretching, while the band at 3655 cm⁻¹ is attributed to the OH stretching.^{19,20} The IR dip spectrum of (1-NpOH)₂ showed vibrational bands at ~3050, 3604, and 3646 cm⁻¹. On the basis of the assignment in 1-NpOH, we assigned the bands around 3050 cm⁻¹ to CH stretching and those at 3604 and 3646 cm⁻¹ to OH stretching. The vibrational bands of the OH stretching are red-shifted by 51 and 9 cm⁻¹ from those in the 1-NpOH monomer. We assigned the band at 3604 cm⁻¹ to the hydrogen-bonded OH moiety and that at 3646 cm⁻¹ to a free OH moiety because the frequency of the OH stretching is

TABLE 1: Observed and Calculated Frequencies of the OH Stretching (cm⁻¹) of (1-NpOH)₂^a

	observed	calculated		
		structure a	structure d	structure e
H-bonded OH moiety	3604		3579	3582
free OH moiety	3646	3647	3638	3639

^a The frequencies are scaled by the factor calculated in the 1-NpOH monomer, 0.956.

TABLE 2. Geometrical Parameters and CP-Corrected Binding Energies D_0 (kcal/mol) of the Structures a–e

	geometrical parameters ^a						binding energy D_0	
	r_1 (r)	r_2	R (x_1, x_2)	x	θ	φ^b		ψ^c
$\pi-\pi$ stacking conformation								
structure a	0.970			3.323	152	5.3	13.5	5.74
structure b	0.969			3.144	138	0.1	1.5	5.33
structure c	0.969		0.717 (x_1) 1.159 (x_2)	3.154		0.0	0.3	4.93
$\pi-\pi$ stacking and hydrogen-bonded conformation								
structure d	0.970	0.974	2.093	3.343		9.1	37.1	5.28
structure e	0.970	0.974	2.074	3.263		8.4	52.5	5.01

^a The units of the geometrical parameters are Å in r , r_1 , r_2 , R , x , x_1 , and x_2 and deg in θ (see Figure 4). ^b The angle between the two naphthalene planes. The unit of φ is deg. The $\varphi = 0$ value means that one naphthalene plane is parallel with another. ^c The torsional angle of the donor OH group with respect to the naphthalene plane. The unit of ψ is deg.

lowered by hydrogen bonding.^{31,32} The observed frequencies of the OH stretching in (1-NpOH)₂ are listed in Table 1 together with the calculated frequencies which will be described later.

C. Stable Isomers of (1-NpOH)₂. We could prepare many derivatives from the naphthalene dimer as the initial geometry. However, we selected five isomers, which are shown in Figure 4a–e, because the geometrical optimization of (1-NpOH)₂ in the MP2/cc-pVDZ calculation was very time-consuming work. The information in Figure 4 is sufficient to discuss the structure of (1-NpOH)₂. As can be seen in the figure, all conformations are of the $\pi-\pi$ stacking type. Moreover, in structures **d** and **e**, the 1-NpOH molecules interact with each other through the O–H...O hydrogen bonding. We also performed the geometrical optimization of (1-NpOH)₂ at the MP2/6-31G(d) level and obtained a hydrogen-bonded chain conformation that is free from the $\pi-\pi$ interaction. The hydrogen-bonded chain conformation, however, changed into the structure **d** in the MP2/cc-pVDZ calculation. It is largely different from the phenol dimer of which the geometry is assigned to be a hydrogen-bonded chain conformation.^{11–17} The geometrical parameters and the CP-corrected binding energies are listed in Table 2. The MP2/cc-pVDZ calculation suggests that the stability of the isomers is in the order of **a** < **b** < **d** < **e** < **c**. The difference in the binding energies among the isomers is within 0.8 kcal/mol. The geometrical parameter x is the intermolecular distance between the aromatic rings of the 1-NpOH molecule. The x values of structures **b** and **c** are smaller than those of structures **a**, **d**, and **e** by ~0.2 Å. This suggests that the contribution for the stabilization by the $\pi-\pi$ interaction is larger in structures **b** and **c** than in structures **a**, **d**, and **e**.

In structures **a–c** the OH moieties of the 1-NpOH molecules are equivalent. The OH bond length of free 1-NpOH monomer is 0.969 Å in the MP2/cc-pVDZ calculation. The OH moieties in structures **a–c** are not assumed to interact with each other, because there is little difference in the OH bond length between the free 1-NpOH monomer and structures **a–c**. In structures **d** and **e**, the 1-NpOH molecules are classified as a proton donor

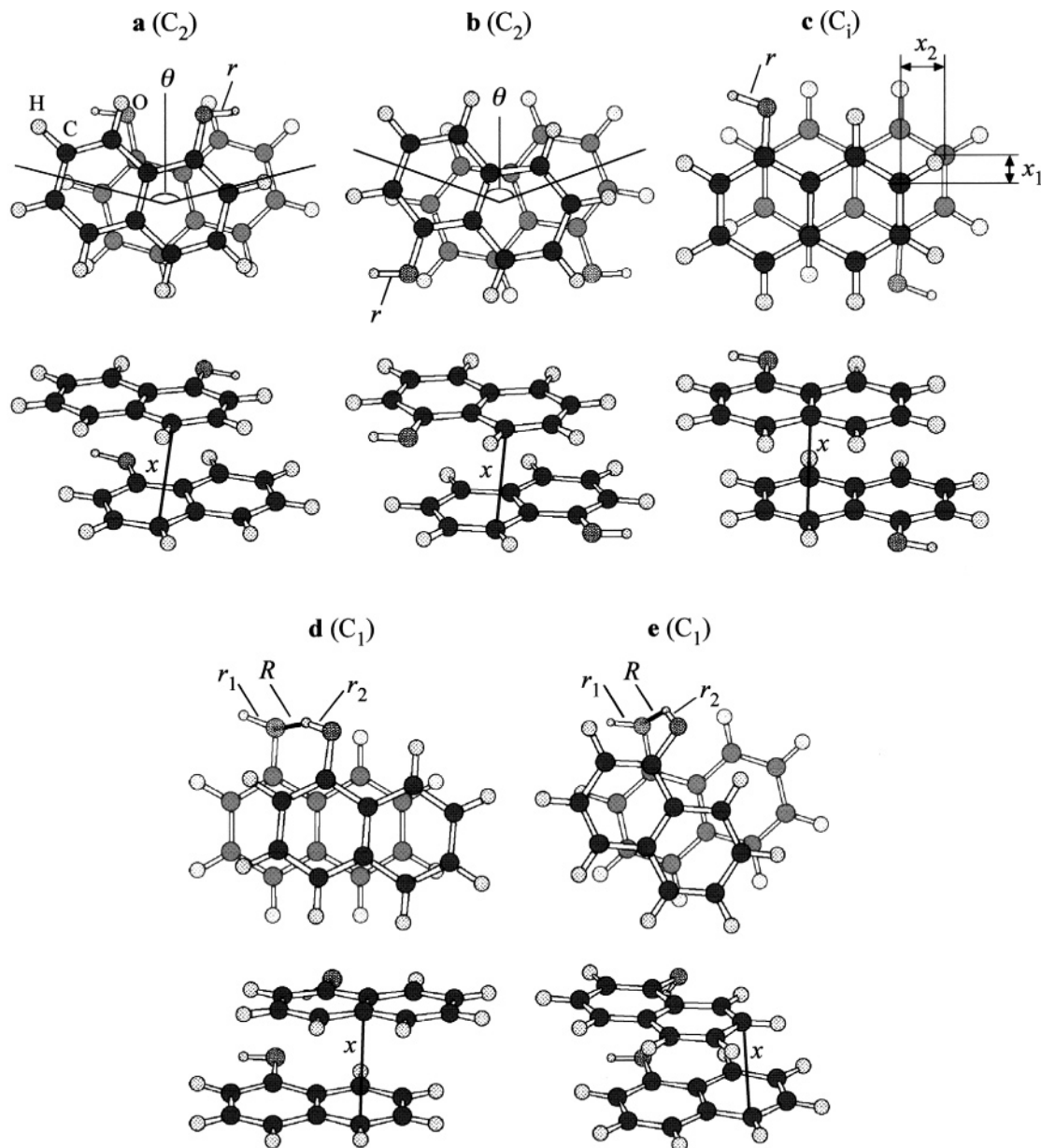


Figure 4. Stable isomers of $(1\text{-NpOH})_2$ in the MP2/cc-pVDZ calculation. The point group is indicated in parentheses.

and acceptor. The OH bond length at the proton-donor site, r_2 , is more elongated than that in the monomer by 0.005 Å.

D. Structural Determination of $(1\text{-NpOH})_2$ Based on the IR Spectrum. We calculated the vibrational frequencies of only structures **a**, **d**, and **e**, because the vibrational analysis of $(1\text{-NpOH})_2$ is very time-consuming. The optimized geometry in Figure 4 suggests that the surroundings of the OH moieties are similar among structures **a**–**c**. Thus, the vibrational spectra of structures **b** and **c** are assumed to be similar to that of structure **a**. Figure 5 shows the calculated IR spectra of structures **a**, **d**, and **e**. The calculated frequencies are listed in Table 1. Figure 5 shows a clear disagreement between the observed spectrum and the calculated one for structure **a**. Only a single OH stretching band is found in the calculated spectrum in structure **a**, while the observed IR spectrum shows two OH stretching bands. On the other hand, the calculated spectra of structures **d** and **e** well reproduce the observed one. On the basis of a comparison between the observed and calculated spectra, we exclude structures **a**–**c** from the candidates, and conclude that the geometry of the observed $(1\text{-NpOH})_2$ cluster is either

structure **d** or structure **e**. It is difficult to distinguish structure **d** or structure **e**, because there is little difference in the calculated frequency of the OH stretching between them.

A comparison between the observed and calculated IR spectra elucidates that structure **a** was not observed in the present experiment, although it was the most stable in the MP2/cc-pVDZ calculation. Several studies have suggested that the MP2/cc-pVDZ calculation is apt to overestimate the binding energy of the π – π interaction.²⁴ We assume that the effect of an overestimation in the case of structure **a** is larger than that in structures **d** and **e**, because the 1-NpOH molecules of structure **a** are bound only by the π – π interaction.

E. Comparison of the Structures between $(1\text{-NpOH})_2$ and $(\text{PhOH})_2$. Structures **d** and **e** suggest that the 1-NpOH molecules are bound by cooperation between the π – π interaction and hydrogen bonding. Such cooperation is absent in the $(\text{PhOH})_2$ cluster, whose geometry is dominated by only hydrogen bonding.^{11–17} A comparison of the structures suggests that the π – π interaction is more enhanced in $(1\text{-NpOH})_2$ than in $(\text{PhOH})_2$. The strength of the hydrogen bonding in $(1\text{-NpOH})_2$

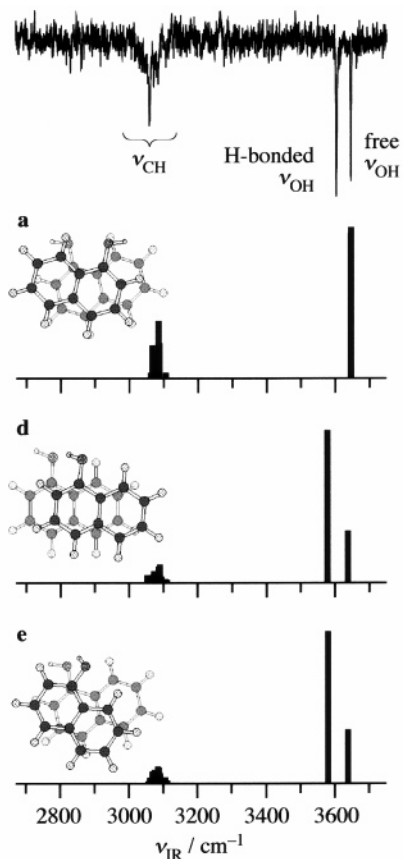


Figure 5. Observed (top) and calculated IR spectra of (1-NpOH)₂ for structures **a**, **d**, and **e**. The structures are illustrated beside the calculated spectra. The observed IR dip spectrum is also shown on the top.

and (PhOH)₂ can be discussed on the basis of the frequency of the hydrogen-bonded OH stretching. The vibrational band of the moiety was red-shifted from that of the free OH one by 51 cm⁻¹ in (1-NpOH)₂ (Table 1) and by 127 cm⁻¹ in (PhOH)₂.^{16,17} A comparison of the shift of the frequency indicates that the hydrogen bonding is weaker in (1-NpOH)₂ than in (PhOH)₂, because the shift of the frequency is proportional to the strength of the hydrogen bonding. Weaker hydrogen bonding in (1-NpOH)₂ is reasonable because the O–H···O hydrogen bond is far from linear in structures **d** and **e** of (1-NpOH)₂. Thus, the different vibrational frequency between (1-NpOH)₂ and (PhOH)₂ also supports structure **d** or **e**.

IV. Conclusions

The structure of the jet-cooled (1-NpOH)₂ cluster was investigated with R2PI and ion-detected IR dip spectroscopy. In the S₁←S₀ R2PI spectrum of (1-NpOH)₂, a partially resolved progression was observed around the origin band. The progression indicates that the intermolecular mode in (1-NpOH)₂ is distorted by photoexcitation. The IR dip spectrum showed two vibrational bands, which were assigned to the hydrogen-bonded and free OH stretching modes. The MP2/cc-pVDZ calculation suggested the existence of five isomers in (1-NpOH)₂. The isomers are classified into a structure dominated only by the π–π interaction and structures formed by cooperation between the π–π interaction and the hydrogen bonding. A comparison of the observed IR spectrum with the calculated ones of the isomers suggests that the geometry of (1-NpOH)₂ is either structure **d** or **e** in Figure 4. We discussed the difference in the

geometrical structures and the vibrational spectra between (1-NpOH)₂ and (PhOH)₂. A comparison of the geometrical structure indicates that the π–π interaction plays an important role only in (1-NpOH)₂, while a comparison of the IR spectra elucidates that the hydrogen bonding is more crucial in (PhOH)₂ than in (1-NpOH)₂. The strong π–π interaction and the relatively weak hydrogen bonding suggest that (1-NpOH)₂ can be depicted as a stacking structure supported by hydrogen bonding.

Acknowledgment. We are grateful to Dr. O. Dopfer (Technische Universität Berlin) for his comments on the ab initio MO calculation of the π–π interaction, and to Professor A. Nakajima (Keio University) for his experimental advice. We also express our gratitude to Professor N. Mikami (Tohoku University) for his support in providing the apparatus. This work is supported in part by a program entitled “Research for the Future (RFTF)” of the Japan Society for the Promotion of Science (No. 98P01203).

References and Notes

- (1) Cantor, C. R.; Schimmel, P. R. *Biophysical Chemistry Part I; the Conformation of Biological Macromolecules*; W. H. Freeman and Company: New York, 1980.
- (2) Guerra, C. F.; Bickelhaupt, F. M.; Snijders, J. G.; Baerends, E. J. *J. Am. Chem. Soc.* **2000**, *122*, 4117.
- (3) Sivanesan, D.; Sumathi, I.; Welsh, W. J. *Chem. Phys. Lett.* **2003**, *367*, 351.
- (4) Hobza, P.; Šponer, J. *J. Am. Chem. Soc.* **2002**, *124*, 11802.
- (5) Jurečka, P.; Hobza, P. *J. Am. Chem. Soc.* **2003**, *125*, 15608.
- (6) Šponer, J.; Hobza, P. *Chem. Phys. Lett.* **1997**, *267*, 263.
- (7) Nir, E.; Kleinermanns, K.; de Vries, M. S. *Natre (London)* **2000**, *408*, 949.
- (8) Nir, E.; Janzen, C.; Imhof, P.; Kleinermanns, K.; de Vries, M. S. *Phys. Chem. Chem. Phys.* **2002**, *4*, 732.
- (9) Plützer, C.; Kleinermanns, K. *Phys. Chem. Chem. Phys.* **2002**, *4*, 4877.
- (10) Bakker, J. M.; Compagnon, I.; Meijer, G.; von Helden, G.; Kabeláč, M.; Hobza, P.; de Vries, M. S. *Phys. Chem. Chem. Phys.* **2004**, *6*, 2810.
- (11) Connell, L. L.; Ohline, S. M.; Joireman, P. W.; Corcoran, T. C.; Felker, P. M. *J. Chem. Phys.* **1992**, *96*, 2585.
- (12) Weichert, A.; Riehn, C.; Brutschy, B. *J. Phys. Chem. A* **2001**, *105*, 5679.
- (13) Riehn, C. *Chem. Phys.* **2002**, *283*, 297.
- (14) Hobza, P.; Riehn, C.; Weichert, A.; Brutschy, B. *Chem. Phys.* **2002**, *283*, 331.
- (15) Ghosh, T. K.; Miyoshi, E. *Theor. Chem. Acc.* **2000**, *105*, 31.
- (16) Ebata, T.; Watanabe, T.; Mikami, N. *J. Phys. Chem.* **1995**, *99*, 5761.
- (17) Hartland, G. V.; Henson, B. F.; Ventura, V. A.; Felker, P. M. *J. Phys. Chem.* **1992**, *96*, 1164.
- (18) Even, U.; Jortner, J.; Noy, D.; Lavie, N. *J. Chem. Phys.* **2000**, *112*, 8068.
- (19) Yoshino, R.; Hashimoto, K.; Omi, T.; Ishiuchi, S.; Fujii, M. *J. Phys. Chem. A* **1998**, *102*, 6227.
- (20) Saeki, M.; Ishiuchi, S.; Sakai, M.; Fujii, M. *J. Phys. Chem. A* **2001**, *105*, 10045.
- (21) Sakai, M.; Daigoku, K.; Ishiuchi, S.; Saeki, M.; Hashimoto, K.; Fujii, M. *J. Phys. Chem. A* **2001**, *105*, 8651.
- (22) Frisch, M. J.; et al. *Gaussian 03*, revision C.01; Gaussian, Inc.: Wallingford, CT, 2004.
- (23) Saeki, M.; Akagi, H.; Fujii, M. *J. Chem. Theory Comput.* **2006**, *2*, 1176.
- (24) Šponer, J.; Leszczynski, J.; Hobza, P. *J. Mol. Struct.: Theochem* **2001**, *573*, 43.
- (25) Del Bene, J. E.; Jordan, M. J. T. *THEOCHEM* **2001**, *573*, 11.
- (26) Boys, S. F.; Bernardi, F. *Mol. Phys.* **1970**, *19*, 553.
- (27) Johnson, J. R.; Jordan, K. D.; Plusquellic, D. F.; Pratt, D. W. *J. Chem. Phys.* **1990**, *93*, 2258.
- (28) Kim, S. K.; Li, S.; Bernstein, E. R. *J. Chem. Phys.* **1991**, *95*, 3119.
- (29) Lakshminarayan, C.; Knee, J. L. *J. Phys. Chem.* **1990**, *94*, 2637.
- (30) Knochenmuss, R.; Muiño, P. L.; Wickleder, C. *J. Phys. Chem.* **1996**, *100*, 11218.
- (31) Ebata, T.; Fujii, A.; Mikami, N. *Int. Rev. Phys. Chem.* **1998**, *17*, 331.
- (32) Zwier, T. S. *Annu. Rev. Phys. Chem.* **1996**, *47*, 205.